*Int. J. Electrochem. Sci.*, 6 **(2011)** 4176 - 4187

International Journal of
ELECTROCHEMICAL
SCIENCE
www.electrochemsci.org

# Platinum Nanoparticles Synthesis Supported in Mesoporous Silica and Its Effect in MCM-41 Lattice

*I. Alonso-Lemus*[1], *Y. Verde-Gómez*[2], *L. Álvarez-Contreras*[*,1]

[1] Departamento de Materiales Nanoestructurados, Centro de Investigación en Materiales Avanzados S. C. Miguel de Cervantes 120, Chihuahua, Chih., México, C.P. 31109.
[2] Departamento de Ingeniería, Instituto Tecnológico de Cancún, Av. Kabah Km 3, Cancún Quintana Roo, México, 77500

[*]E-mail: lorena.alvarez@cimav.edu.mx

*Received:* 7 June 2011 / *Accepted:* 25 July 2011 / *Published:* 1 September 2011

Platinum nanoparticles were incorporated in MCM-41 mesoporous support. Two different ways to incorporate metallic nanoparticles were evaluated (i) Pt wetness impregnation in MCM-41 previously synthesized and (ii) Pt incorporated in situ during MCM-41 synthesis in alkaline (iia) and acid (iib) media. Synthesis conditions influence was studied by X-Ray diffraction, nitrogen adsorption analysis and electron microscopy. High surface areas (up to 900 $m^2/g$) were obtained in all methods. However, high Pt loading were observed only in wetness impregnation and in situ incorporation in alkaline media methods. Additionally, composites Pt/MCM-41-black carbon were prepared and their electrocatalytic activity and electrical bulk resistance were studied by cyclic voltammetry (CV) and electrochemical impedance spectroscopy (EIS), respectively. An interesting behaviour was observed in the samples where the platinum was in situ incorporated; the samples show structural and textural properties modifications compared to raw MCM-41.Hydrogen oxidation reaction by CV was observed in high Pt loading samples. On the other hands, EIS results indicate that Pt/MCM-41 materials synthesized by in situ incorporation methods have lower electrical bulk resistance than the samples prepared by wetness impregnation method.

**Keywords:** Electrocatalyst, MCM-41, mesoporous support, impedance spectroscopy, platinum nanoparticles.

## 1. INTRODUCTION

MCM-41 and MCM-48 materials are mesoporous molecular sieves widely used in nanoscience [1, 2]. These materials have considerable interest in gas adsorption applications [3-5], catalyst supports

[6, 7] and adsorbents in separation processes such as HPLC and supercritical fluid chromatography [8]. Support materials in catalyst have a strong influence on the properties of active phase. Noble metal particles usually play an important role as active phase, which has a direct impact on the catalyst cost.

Many methods have been development in order to increase the nanoparticles dispersion and reduce the metal loading [9-20]. The most widely techniques used in several catalytic applications are impregnation method [9-11], colloidal method [12-16] and recently microemulsion method [17-19]. Above methods include a chemical step to form nanoparticles, followed by deposit step to disperse active phase on support [20]. On the other hand, direct incorporation of the metallic phase during support synthesis is an alternative route to obtain supported metal nanoparticles with the advantage of being a one-step method.

Electrocatalysis area has many technological challenges in which metallic nanoparticles synthesis could be used to develop tailor materials [20]. Conventionally, carbon particles are used as electrocatalyst supports, because their relative stability in acidic and basic media, textural properties and good electronic conductivity. Carbon blacks as Acetylene Black [22, 23], Ketjen Black [24] and Vulcan XC-72 [22,23,25] are some examples of carbonaceous materials used in electrocatalytic applications. In recent years, carbon nanotubes (CNTs) and mesoporous ordered carbon were explored as nanostructured catalysts supports. CNTs have shown very promising results in electrochemical devices applications [26-29] Modified MCM-41 shows some advantages over carbon-based support such as better chemical stability, ionic conductivity, higher surface area and acid surface. Additionally, MCM-41 has not diffusion problems due to their ordered mesoporous structure. MCM41 properties suggest its exploration in electrocatalytic applications.

In this work metallic platinum nanoparticles were synthesized and supported on MCM-41 in two different ways, Pt wetness impregnation in MCM-41 previously synthesized and Pt incorporated in situ during MCM-41 synthesis in different aqueous media. Pt/MCM-41 materials obtained were characterized by X Ray Diffraction (XRD), adsorption nitrogen analysis and electron microscopy. Additionally electrochemical test were performed in order to evaluate the electrocatalytic activity and materials bulk resistance.

## 2. EXPERIMENTAL

### *2.1. Synthesis of Pt/MCM-41 materials*

The synthesis of Pt/MCM-41 materials was carried out in two different ways (i) Pt wetness impregnation in MCM-41 previously synthesized and (ii) Pt incorporated in situ during MCM-41 synthesis in alkaline (iia) and acid (iib) media.

#### *2.1.1. Wetness Impregnation*

MCM-41 mesoporous material was synthesized prior to catalyst incorporation as follows: Sodium aluminate ($NaAlO_2$, 99.95%, Riedel-de Haën), as the aluminium source, and

cetyltrimethylammonium bromide (CTAB, 99%, Alfa Aesar), as the organic template, were dissolved in ammonium hydroxide solution ($NH_4OH$, 30%, Aldrich). The mixture was stirred until a clear solution was obtained. Then, tetraethyl orthosilicate (TEOS, 98%, Aldrich) as silica source was added. The solution was stirred at room temperature during 24 hours. The final solution molar ratio was: 1Si/0.05Al/0.9CTAB/4056$H_2O$/264$NH_4OH$. Synthesis product was recovered by filtration and washed with distillated water. Powders were calcined in air at 550 ˚C for 4 hours.

Aqueous solution of ammonium hexachloroplatinate ((NH4)2PtCl6, 99.9%, Alfa Aesar) was used as Pt precursor. Platinum solution was incorporated drop by drop on MCM- 41. Then, the material was dried at 100 ˚C. The sample was called WI.

### *2.1.2. Pt incorporated in situ in alkaline media*

Alkaline media synthesis (ALK) was performed incorporating platinum precursor in the course of MCM-41 synthesis. $NaAlO_2$, CTAB and $(NH_4)_2PtCl_6$ were dissolved in $NH_4OH$ solution. The mixture was stirred until a yellowish solution was obtained, then, TEOS was added. Molar ratio was 1Si/0.05Al/0.9CTAB/4056$H_2O$/264$NH_4OH$/0.018Pt. Solution was maintained by stirring for 24 hours at 60 ˚C and atmospheric pressure. Synthesis products were recovered by filtration and heat-treated as previous sample.

### *2.1.3. Pt incorporated in situ in acid media*

This synthesis was carried out dissolving hydrochloridic acid (HCl, 38%, J.T. Baker), $(NH_4)_2PtCl_6$ and CTAB in distilled water and stirred for 2 hours. TEOS was added drip and stirring again during 1 hour. Solution has the following molar composition 1Si/6.35CTAB/1495$H_2O$/180HCl/0.013Pt. The mixture was heated at 80 ˚C in static Teflon-lined reactor under autogenous pressure for 7 days. Final solid product was filtered, washed with distilled water and dried at 100 ˚C during 2 hours. Powder was calcined at 550 ˚C for 4 hours. This sample was called ACD.

Finally, three synthesized materials were treated in reductive atmosphere ($H_2/N_2$ mixture) at 400 ˚C during 4 hours. Theoretical metal loadings were 5% wt. Pt/MCM-41.

### *2.2. Characterization*

Samples were characterized by X Ray diffraction (XRD) to determine the MCM-41 mesoporous structure and Pt crystallite size. Measurements were carried out at room temperature on a Panalytical X´PertPRO, using CuKα-1 radiation (40kV, 30 mA) and X´Celerator accessory; the step size was 0.016° and 24.13 s per step. The $d_{spacing}$ parameters were determined using High score software directly from XRD patterns.

Textural properties such as surface area, porous size distribution and porous shape were performed by nitrogen adsorption analysis using a Quantachrome Autosorb-1 with high purity nitrogen

as adsorbate. Prior determinations of the adsorption isotherms, the samples were outgassed for 5 h at 300 ˚C. Surface area was obtained by multipoint BET method.

In order to know elemental composition and metal loading on MCM-41, energy dispersive spectroscopy (EDS) technique was used. Analysis were determined using EDAX Prime equipment coupled to Scanning Electron Microscope JEOL 5800 LV. Microanalyses were randomly taken in several sample zones at low magnification in order to have a representative value of the elemental composition.

Morphology was determined using Philips CM-200 Transmission Electron Microscope (TEM) and JEOL7410 (5.0 kV) Scanning Electron Microscope (SEM). TEM and SEM specimens were prepared by dispersing the sample in ethanol by ultrasound for 5 minutes. A drop of the suspension was placed into a holey carbon Cu grid and was allowed to dry.

### *2.3. Electrochemical measurements*

Electrochemical characterization was conducted using a glassy carbon disk electrode (0.07 $cm^2$). Catalyst suspension was sonicated during 30 minutes with the following composition; Pt/MCM-41 material and Vulcan XC72 (Cabot Corporation) with 1:1 weight ratio were dispersed in distilled water (suspension concentration = 10 mg/mL). Catalyst films were fixed on disk electrode with 5μL aliquot of 20:1 distilled water:Nafion® solution and allowed to dry at room temperature inside a dessicator. Electrochemical measurements were carried out at room temperature using a Princeton Applied Research VersaSTAT$^3$ potentiostat/galvanostat. A conventional three-electrode cell, oxygen free (purged and blanked with argon) was used with a saturated calomel electrode (SCE: $Hg/Hg_2Cl_2$/sat. KCl) as reference electrode and platinum foil as counter electrode. Cyclic voltammetry (CV) and electrochemical impedance spectroscopy (EIS) studies were performed in 0.5 M sulfuric acid ($H_2SO_4$, 98%, J.T. Baker) electrolyte solution saturated with argon. CV was carried out at potential range from -0.3 to 0.6 V vs. SCE and scan rate of 20 $mVs^{-1}$. EIS spectra were obtained at open circuit potential by applying 10 mV sinusoidal signal. Frequency range was from 100 KHz to 100 mHz.

## 3. RESULTS AND DISCUSSION

### *3.1. Structural Features*

MCM-41 and Pt/MCM-41 diffraction patterns at low and high angles are shown in Figure 1a and 1b, respectively. Three characteristics peaks of hexagonal array materials can be observed at low angles region, corresponding to the planes (100), (110) and (200) [2]. The $d_{spacing}$ parameter associated to (100) peak shift can be directly related to pore size modification. Insert in figure 1a shows the $d_{spacing}$ value from each sample. ALK and ACD samples present larger pore size than WI sample. Pore size modification may be occurring due to the in situ platinum incorporation has an effect on the silica lattice.

Diffraction patters at high angles (Figure 1b) show the characteristic peaks of FCC Pt phase at (111), (200), (220), (311) and (222) planes.

**Table 1**. Physicochemical and electrochemical features of Pt/MCM-41 materials.

| Sample | Scherrer Pt crystallite size (nm) | Pt load (%wt.) | BJH pore size (nm) | $S_{BET}$ ($m^2/g$) | EAA ($m^2/g$) | Charge transfer resistance (KΩ) |
|---|---|---|---|---|---|---|
| MCM-41 | - | - | 2.4 | 1272 | - | - |
| WI | 42 | 5.50 | 2.4 | 904 | 2 | 117 |
| ALK | 16 | 5.78 | 2.7 | 1078 | 8 | 14 |
| ACD | 23 | 0.31 | 2.7-8.1 | 1047 | 0 | 17 |

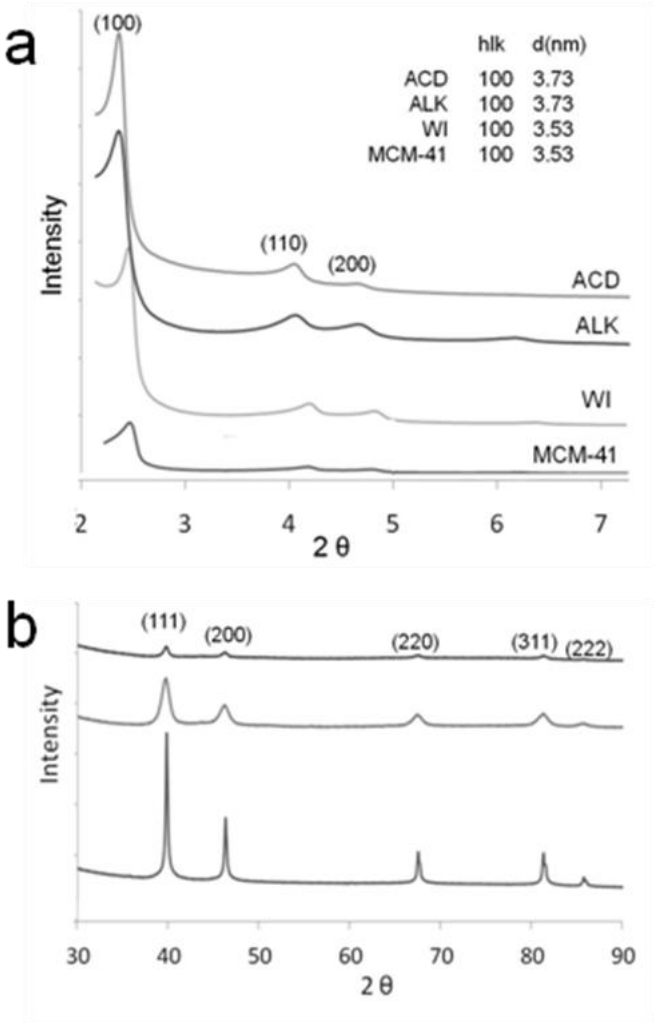


**Figure 1**. Pt/MCM41 XRD Patterns a) at low angles and b) at high angles

Moreover, no additional peaks were observed, which indicate the absence of any crystalline phase containing aluminum or another platinum phase [30]. XRD results suggest two ways of platinum incorporation in the samples synthesized by in situ method (ALK and ACD ): (i) the platinum metallic nanoparticles were deposited on MCM-41 support and, (ii) a low quantity of platinum could be incorporated into the MCM-41 lattice ((100) peak shift ). Platinum crystallite size was determinate by Scherrer equation [31] from XRD patterns using the (111) peak in all samples and summarized in Table 1. The broad nature of the peaks indicates very small Pt crystallite size in all samples. Although the incorporation in situ methods was performed in two different media, particle sizes obtained were very similar (16 and 23 nm). These crystallites sizes are smaller than those obtained by WI method (42 nm).

### *3.2. Textural properties.*

Surface area, porous shape and pore size distributions (PSD) were calculated from adsorption nitrogen analysis.

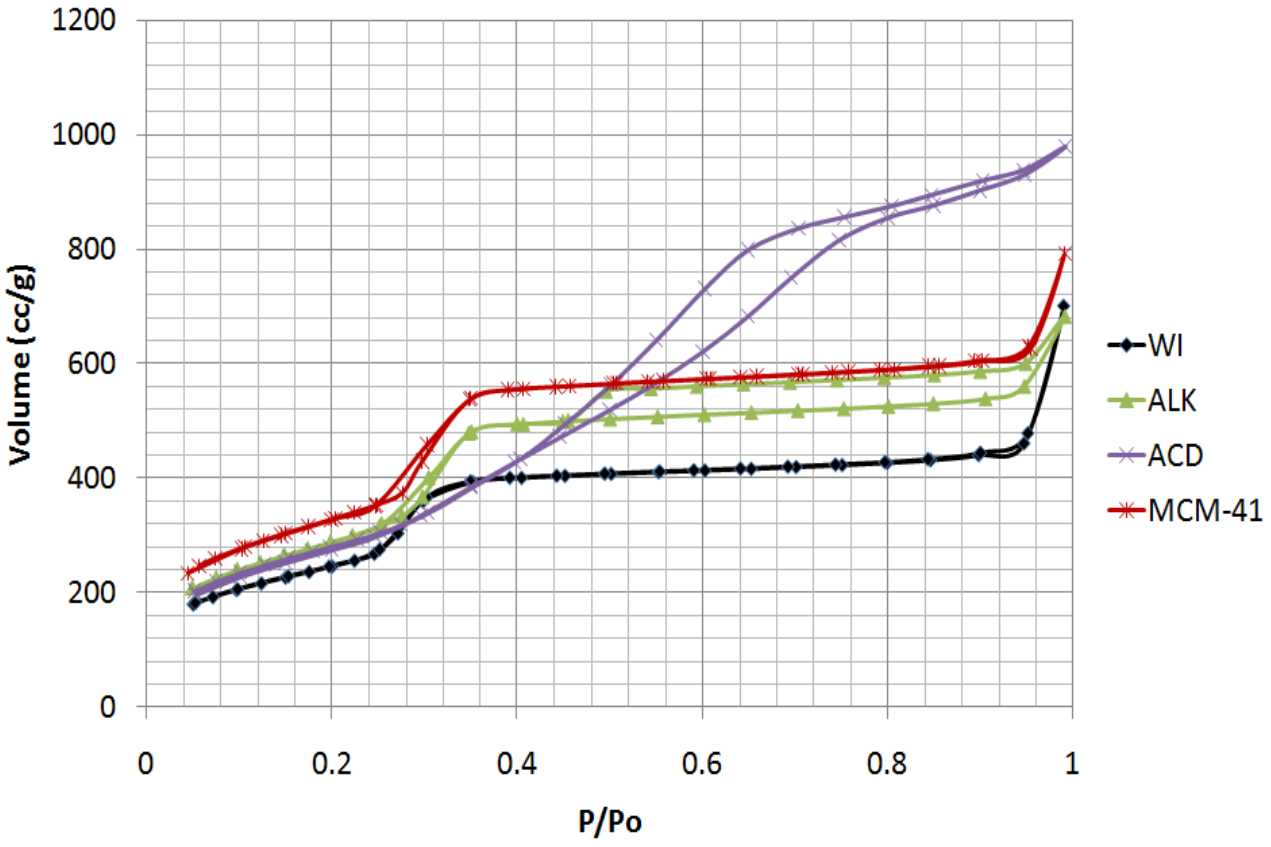


**Figure 2**. $N_2$ Adsorption-desorption isotherms and pore size distribution (insert) of Pt/MCM41 materials and MCM-41

Figure 2 shows nitrogen isotherms and BJH pore size distribution for Pt/MCM-41 materials and raw MCM-41. All isotherms obtained are type IV that is characteristic of mesoporous materials with uniform array [30]. WI and MCM-41 samples show isotherms without hysteresis loop typical of materials with cylindrical pores [31]. Also, PSD is very similar in both samples as expected. A decrease in surface area was observed in WI sample (904 $m^2/g$) with respect to raw MCM-41 (1272 $m^2/g$), possibly to the platinum nanoparticles pore blocking in WI sample.

ALK and ACD textural properties show interesting results. For example, ALK has high surface area (1078 $m^2/g$) and hysteresis loop type H4, which is commonly associated with narrow slit-like arrays pores [32]; additionally PSD indicate a narrow distribution pore size near to 2.7 nm. ACD sample also show high surface area (1047 $m^2/g$) with wide distribution PSD (2.7-8.1 nm) and hysteresis loop type H2, which was attributed to the "ink bottles" shaped pores; however, the role of network effects must be also taken into account [32]. ALK and ACD pore size result is in agreement with the shift peak in XRD, which confirm a pore size modification due to the platinum in situ incorporation.

Although all samples shows high surface areas ($\leq$ 900 $m^2/g$), samples ALK and ACD have approximately 150 $m^2/g$ higher surface area than WI sample. It means that in situ platinum incorporation improves surface area value.

### *3.3. Elemental analysis*

Platinum loading was determined by EDS (Table 1). 5% wt Pt loading was found in ALK and WI samples. This result indicates very high platinum incorporation efficiency with zero losses (100% yields). Previous works showed that platinum incorporation by in situ methods presented low efficiency loadings (up to 3% wt) [33]. High yield result in ALK sample is observed due to the platinum precursor has higher solubility in alkaline media than in acid media. Hereby ACD sample has a very low platinum incorporation (0.3% wt Pt, determined by ICP technique). The advantage in wetness impregnation is to ensure the high target loading through the addition of the all metal precursor solution; however, during the impregnation process, many factors can affect the composition, morphology and catalyst dispersion, which could be influence the catalytic activity [20].

### *3.4. Morphology.*

Figure 3 shows SEM micrographs obtained from synthesized samples.

Morphologies found in WI (Fig. 3a) and ALK (Fig.3b) samples were very similar, as expected, since both syntheses were done in alkaline media. Cloud-like crystals agglomerates were observed in these samples with size near to 500 nm. ACD sample shows crystals between 2000 to 4000 nm in the form of gyroids. It has been reported that the morphology was easier to change under acidic conditions due to the interaction between surfactant and silica framework is weaker [34-36], hence the difference between ACD and ALK morphology. In order to observe platinum nanoparticles, TEM technique was employed.

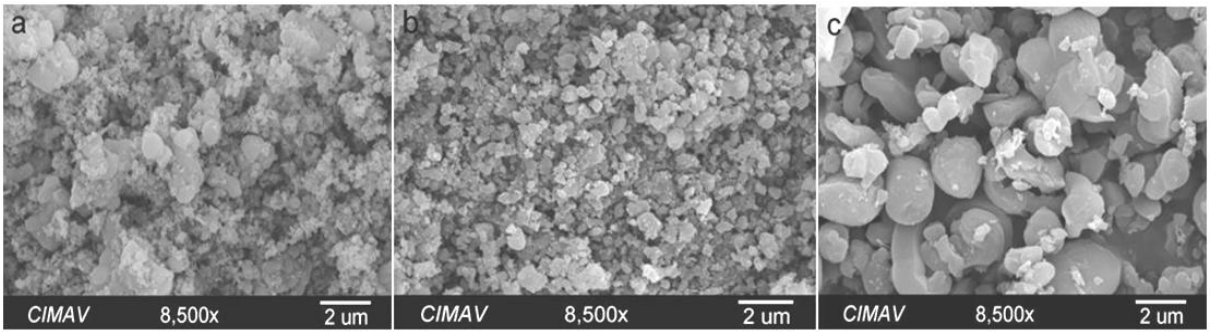


**Figure 3**. SEM Images of Pt/MCM-41 materials, A) WI sample, B) ALK sample and, C) ACD sample

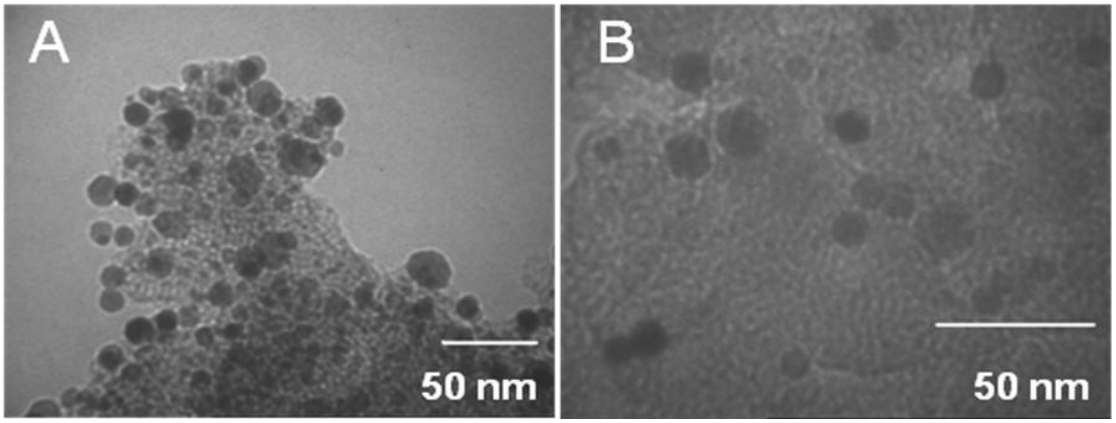


**Figure 4.** TEM Images of Pt/MCM-41, A) Wi sample and B) ALK sample.

Figure 4 shows ALK and WI samples, platinum nanoparticles in spherical shape were observed in both samples. WI sample (Figure 4a) has platinum nanoparticles around 10 to 35 nm, while ALK sample shows platinum nanoparticles between 7 to 13 nm. These results are in agreement with the particle size calculated by Scherrer equation. Previous studies suggest that Pt nanoparticles supported on mesoporous materials based-silica improve the catalyst performance in oxidation reactions [37]; hence, Pt/MCM-41 materials synthesized in alkaline media could find several application fields given the simplicity of the synthesis method and their properties.

In ACD sample case was not possible to observe platinum nanoparticles, due to the synthesis conditions makes difficult the platinum incorporation.

### *3.5. Electrochemical performance*

#### *3.5.1. Electrochemical Impedance Spectroscopy (EIS)*

EIS is a technique commonly used to calculate electrical resistances in bulks materials obtained from the Nyquist plot [38, 39]; then, each circuit component is associated with a phenomenon

occurring inside the electrochemical cell in which the test is performed. The Nyquist plot shows a semicircle curve for all samples (Figure 5). These curves were adjusted at equivalent circuit shown in Figure 5 insert. The equivalent circuit is composed of the following components: electrolyte resistance (Rs), charge transfer resistance in the material bulk (R1) and the constant phase element (CPE) commonly associated to a no ideal capacitive behaviour. R1 values obtained in each sample are shown in Table 1.

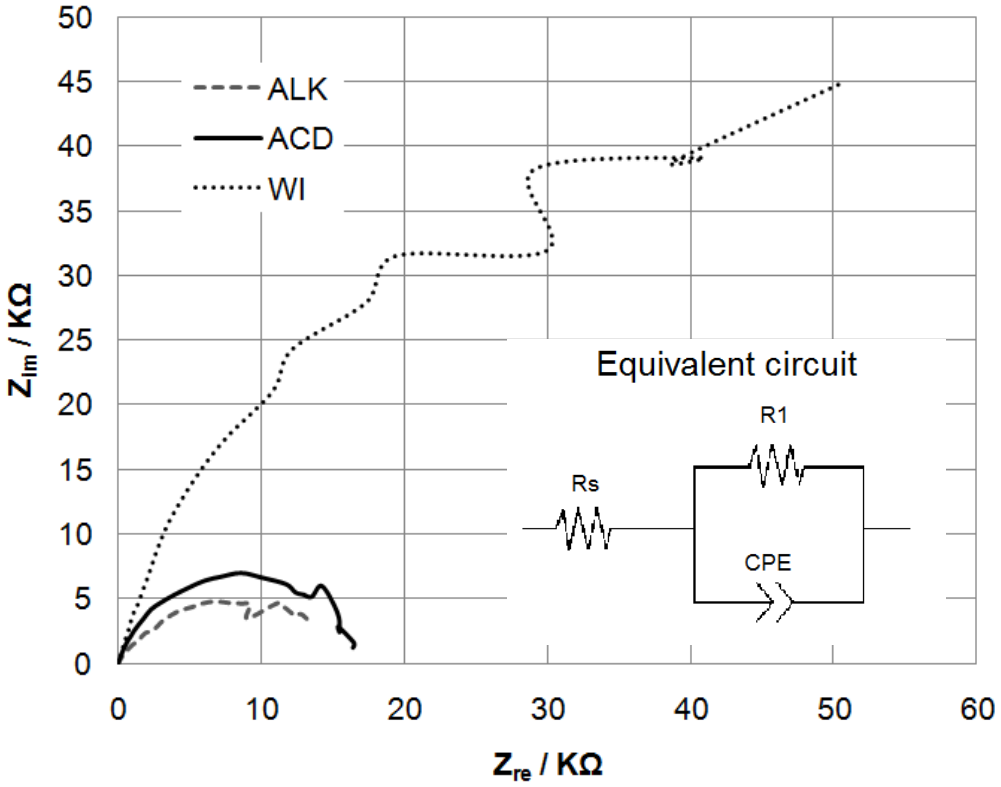


**Figure 5.** Nyquist diagram and equivalent circuit of Pt/MCM41materials.

ALK and ACD samples show a very close R1 value (14 and 17 kΩ, respectively), while WI sample has a higher R1 value (114 kΩ). This suggests that the platinum incorporation method has influence on the charge transfer resistance of the support lattice. ALK and ACD were synthesized incorporating platinum during the synthesis of the MCM-41 support.

### *3.5.2. Electrocatalytic activity*

The cyclic voltammetry (CV) technique was used to obtain the electrochemical active area (EAA) for the Pt/MCM-41 materials. CV is commonly used to obtain the electrical charge required for the adsorption and desorption of the H2 in Pt (QH), and therefore to determine the EAA in the catalysts based on Equation 1 [40].

$$EAA = QH / (QHo\ GMe) \quad (1)$$

where QHo is the charge required for oxidation of a single molecule of H2 on a polycrystalline Pt surface of 1 cm2 (0.21 mC/cm2) [41]. GMe is the metal loading in the working electrode. The GMe was calculated from EDS analysis.

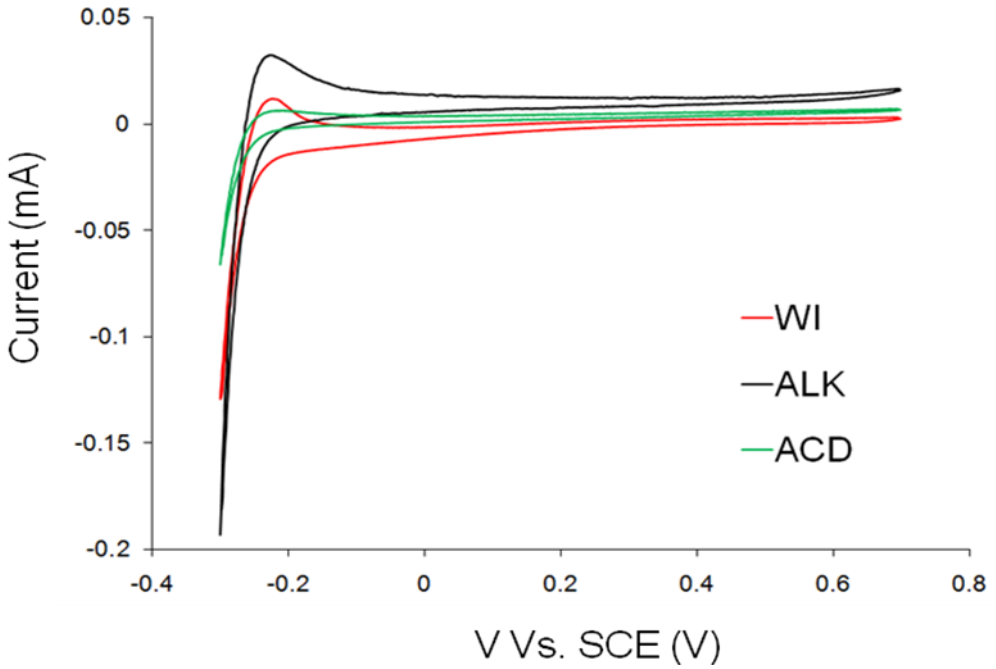


**Figure 6.** Cyclic Voltammograms of Pt/MCM41 samples. Half cell test was performed in 0.5 M $H_2SO_4$ at scan rate of 20 mV/s in Ar atmosphere.

Figure 6 shows the CV curves obtained from the all samples and the EAA calculated in each case is presented in Table 1. The results suggest that the hydrogen oxidation occur easily on platinum surface supported on WI and ALK materials (EAA = 2 and 8 m2/g, respectively). WI has lower EAA than ALK sample since they have the same metal loading. This could be due to the following two reasons; first, Pt particle size was smaller in ALK than in WI sample; so, more platinum surface area is available in ALK sample to act as an electrocatalyst; in second place, the effect of the electron transfer due to the charge transfer resistance is lower in the ALK sample than in the WI sample. On another hand, the ADC sample does not show EAA because of the Pt loading was too low to carry out the hydrogen reaction. .

EAA calculated for ALK and WI samples is lower than commercial material (e.g. 20% wt. Pt/C, ETEK. EAA~50-60 $m^2/g$ [42, 43]. The low electrochemical performance in Pt/MCM-41 materials is due to the following reasons: (i) platinum loading in the WI and ALK samples is lower than carbonaceous materials (approximately 4 times); and (ii) platinum particle size in Pt/MCM-41 is bigger than Pt/C (~ 3nm). However, considering the novel properties, simplicity in the synthesis and potential to be modified in order to improve the platinum dispersion and particle size, with the consequence a better electrochemical performance, Pt/MCM-41 is a good candidate to be considered as electrocatalyts in electrochemical devices.

## 4. CONCLUSIONS

Pt-MCM41 samples were prepared by three different synthesis methods. Structural features and textural properties suggest that mesoporous structure were conserved since the platinum incorporation in all samples, The samples where the platinum was incorporated by in situ synthesis, size and shape of the pore were modifying, which indicate that platinum influences on MCM-41 lattice.

High metal incorporations yields were obtained in the WI and ALK samples. This behaviour is attributed to the platinum precursor nature, which is more soluble in alkaline solutions than acid solutions. Pt particles size observed by TEM are in agreement with the Scherrer calculations in samples ALK and WI; however in ACD sample Pt nanoparticles were not observed due to the low platinum incorporation. Finally, electrochemical tests were performed in order to know the electrocatalytic activity and charge transfer resistance in the material bulk. Electrocatalytic activity was only detected in the WI and ALK samples where the platinum loading was close to 5% wt. The low charge transfer resistance found in ACD and ALK suggest that platinum incorporated by in situ methods has influence on MCM-41 lattice which is in agreement with XRD and textural properties results. According to the results, Pt/MCM-41 could be considered as a good electrocatalyst candidate for electrochemical applications, such as fuel cells and sensors.

ACKNOWLEDGEMENTS
This work was supported CONACyT Project 26067, the authors were gratefully for financial support and we would like to be are grateful for the valuable technical assistance from Enrique Torres and D. Lardizabal.

## References

1. C.T. Kresge, M. E. Leonowicz, W. J. Roth, J. C. Vartuli and J. S. Beck, *Nature* 359 (1992) 710.
2. J. S. Beck, J. C. Vartuli, W. J. Roth, M. E. Leonowicz, C.T. Kresge, K. D. Schmitt, C. T. –W. Chu, D. H. Olson, E. W. Sheppard, S. B. McCullen, J. B. Higgins and J. L. Schlenker, *Am. Chem. Soc*. 114 (1192)10834.
3. R. Schmitt, M. Stöcker, E. Hansen, D. Akporiaye and O. H. Ellestad, *Micropor. Mater* 3 (1195) 443.
4. P. J. Branton, P. G. Hall, K. S. W. Sing, *J. Chem. Soc. Chem. Commun* (1993) 1257.
5. P. L. Llewellyn, F. Schüth, Y. Grillet, F. Rouquero, J. Rouquero, K. K. Unger, *Langmuir* 11 (1195) 574.
6. L. Li, P. Wu, Q. Yu, G. Wu, N. Guan, *Appl. Catal. B Environ*. 94 (2010) 254.
7. U. Junges, W. Jacobs, I. Voigt-Martin, B. Krutzsch, F. Schüth, *J. Chem. Soc. Chem. Commun* (1995) 2283.
8. M. Grün, A. A. Kurganov, S. Schacht, F. Schüth, K. K. Unger, J, *Chromatogr. A*, 710 (1996) 1.
9. Y. Zhang, A.M. Valiente, I.R. Ramos, Q. Xin, A.G. Ruiz, *Catal. Today*, 93–95 (2004) 619.
10. C.W. Hills, N.H. Mack, R.G. Nuzzo, *J. Phys. Chem. B*, 107 (2003) 2626.
11. J.T. Moore, J.D. Corn, D. Chu, R. Jiang, D.L. Boxall, E.A. Kenik, C.M. Lukehart, *Chem. Mater*. 15 (2003) 3320.
12. U.A. Paulus, U. Endruschat, G.J. Feldmeyer, T.J. Schmidt, H. Bönnemann, R.J. Behm, *J. Catal.* 195 (2000) 383.
13. H. Bönnemann, R. Brinkmann, S. Kinge, T.O. Ely, M. Armand, *Fuel Cell*, 4 (2004) 289.

14. M.T. Reetz, M.G. Koch, *J. Am. Chem. Soc*. 121 (1999) 7933.
15. X. Wang, I. Hsing, *Electrochem. Acta* 47 (2002) 2897.
16. T. Kim, M. Takahashi, M. Nagai, K. Kobayashi, *Electrochem. Acta* 50 (2004) 813.
17. J. Solla-Gullon, F.J. Vidal-Iglesias, V. Montiel, A. Aldaz, *Electrochim. Acta* 49 (2004) 5079.
18. L. Xiong, A. Manthiram, *Solid State Ionics* 176 (2005) 385.
19. S. Rojas, F.J. Garcia, S. Jaras, M.V. Huerta, J.L.F. Fierro, M. Boutonnet, *Appl. Catal. A: Gen.* 285 (2005) 24.
20. H. Liu, C. Song, L. Zhang, J. Zhang, H. Wang and D. P. Wilkinson, *J. Power. Sources* 155 (2006) 95.
21. H. Hamad, T. Hamieh, H. Mahzoul, J. Toufaily. *Adv. Powder Technol* 19 (2008) 131.
22. M. Uchida, Y. Aoyama, M. Tanabe, N. Yanagihara, N. Eda, A. Ahta, *J. Electrochem. Soc.* 142 (1995) 2572.
23. E. Antoli, R.R. Passos, E.A. Ticianelli, *J. Power Sources* 109 (2002) 477.
24. A.S. Arico, S. Srinivascan, V. Antonucci, *Fuel Cells* 2 (2001) 133.
25. H. Lui, C. Song, L. Zhang, J. Zhang, H. Wang and D.P. Wilkinson, *J. Power Sources* 155 (2006) 95.
26. C. Wang, M. Waje, X. Wang, J.M. Tang, R.C. Haddon, Y. Yan. *Nano Lett.* 4 (2004) 345.
27. T. Matsumoto, T. Komatsu, K. Arai, T. Yamasaki, M. Kijima, H. Shimizu, Y. Takasawa, J. Nakamura, *Chem. Commun* (2004) 840.
28. W. Li, C. Liang, W. Zhou, J. Qiu, H. Li, G. Sun, Q. Xin, *Carbon*, 42 (2004) 436.
29. Y. Verde, A. Keer, M. Miki, F. Paraguay, M. Avalos and G. Alonso, *J. Fuel Cell Sci. Tech* 4 (2007) 130.
30. M.M.L. Ribeiro Carrott, F.L. Conceicao, J.M. Lopes, P.J.M. Carrott, C. Bernardes, J. Rocha, F. Ramoa Ribeiro. *Micropour. Mesopour. Mat*. 92 (2006) 270.
31. B. E. Warren, *X-Ray Diffraction*, Addison-Wesley, Reading, MA. (1996)
32. K. S. W. Sing, D. H. Everett, R. A. W. Haul, L. Moscou, R. A. Pierotti, J. Rouquerol, T. Siemieniewska. *Pure & Appli. Chem*, 57 (1985) 603.
33. L. Jiao, J.R. Regalbuto, *J. Catal*. 260 (2008) 342.
34. C.G. Sonwane, P.J. Ludovice. *J Molec. Catal. A: Chem* 238 (2005) 135.
35. H.P. Lin, S.B. Liu, C.Y. Mou, *Chem. Commun* (1999) 583.
36. H. Yang, N. Coombs, I.N. Sokolove, G.A. Ozin, *Nature* 381 (1996) 589.
37. A.Taguchi, F. Schüth. *Micropour. Mesopour. Matter* 77 (2005) 1.
38. H. Yang, A. Kuperman, N. Coombs, S. Mamiche-Afara, G.A. Ozin, *Nature* 379 (1996) 703.
39. K.R. Cooper and M. Smith, *J. Power Sources* 160 (2006) 1088.
40. Pozio, A., M. De Francesco, A. Cemmi, F. Cardellini, L. Giorgi. *J. Power Sources* 105 (2002) 13.
41. M.R. Tarasevich, V.A. Bogdanovskaya, B.M. Grafov, N.M. Zagudaeva, K.V. Rybalka, A.V. Kapustin, Y.A. Kolbanovskii, Russ. *J. Electrochem.* 41 (2005) 746.
42. E.A. Ticianelli, J.G. Beery, S Srinivasan, *J. Appl. Electrochem*. 21 (1991) 597.
43. J. Perez, E.R. Gonzalez, E.A. Ticianelli, *Electrochim. Acta* 44 (1998) 1329.